Appendix 1: $^{40}Ar/^{39}Ar$ Methods and Data:

Structure and $^{40}Ar/^{39}Ar$ K-feldspar Thermal History of the Gold Butte Block: Re-evaluation of the Tilted Crustal Section Model

Karlstrom, K.E., Heizler, M., and Quigley, M.C.

$^{40}Ar/^{39}Ar$ METHODS AND AGE CALCULATIONS

Mass spectrometry

All of the samples and standards were analyzed for argon isotopic composition with an MAP-215-50 mass spectrometer equipped with a Johnston electron multiplier. The multiplier is operated at about 2.2 kV and yields a gain above the Faraday collector (10E11 ohm resistor) of about 7000. Typical sensitivity values were 1.0-2.5e-16 mol/pA and 1.0e-16 mol/pA for the furnace and laser systems, respectively. Resolution at 5% peak-height at mass 40 was typically 600. Additional information about the New Mexico Geochronology Research Laboratory can be found within New Bureau of Geology and Mineral Resources open file report OF-AR-1 at http://geoinfo.nmt.edu/publications/openfile/argon/home.html.

Furnace Step-Heating:

All of the unknowns were step-heated in a double vacuum Mo resistance furnace. Heating times for the K-feldspars were highly variable (10-475 min) and are designed to maximize recovery of the diffusion coefficients and to resolve excess argon contamination by performing several isothermal replicate-heating steps. Heating time for muscovite, biotite and hornblende was 7 minutes for each step. All furnace samples were gettered during heating using a SAES GP-50 getter operated at ~450°C. Following heating, gas was expanded to a second-stage of the extraction line where it was reacted with 2 GP-50 getters (one at 20°C, one at ~450°C) and a W filament operated at about 2000°C. Typical K-feldspar gettering time in the second stage was 2 minutes, whereas

biotite and hornblende were gettered for 5 minutes. The furnace thermocouple was calibrated by melting copper foil and typically the recorded temperature underestimated the sample temperature by 60-100°C. For the K-feldspar data, correction of thermocouple temperature to the Cu foil melting point was done on a sample-by-sample basis and the reported temperature in the data table is calibrated to the foil melting. Estimated accuracy of the heating temperature is ±15°C for any given step.

Blanks and backgrounds for the K-feldspars were typically determined during a 15-minute, 800°C blank run. For the long and higher temperature heating steps this method under-corrects the true blank and therefore the reported radiogenic yield for these steps contains atmospheric argon that is not solely derived from the samples. Because of the age and high K-content of the K-feldspars, the blank contribution is very minor as reflected by the very high radiogenic yields for all heating steps. Blanks for the micas and hornblende were run before, during and after the step heating and typically yielded values of $2x10^{-15}$, $1.2x10^{-17}$, $5x10^{-18}$, $4x10^{-18}$, and $8x10^{-18}$ moles for masses 40, 39, 38, 37 and 36, respectively.

Laser Total Fusion for Fish Canyon flux monitor:

Single sanidine crystals were fused with a Synrad 50 W CO_2 laser during a 20 second heating with a focused 1.6 W laser. Extracted gas was cleaned for 2 minutes using 2 GP-50 getters (one at 20°C, one at ~450°C), a W filament operated at about 2000°C and reaction with a cold finger operated at –140°C. Blanks plus backgrounds for were typically: $1x10^{-16}$, $3\ x10^{-18}$, $1\ x10^{-18}$, $4\ x10^{-18}$, and $2x10^{-18}$ moles for masses 40, 39, 38, 37 and 36, respectively.

Irradiations, Flux monitoring and age calculations:

Irradiations were preformed at both the University of Michigan Ford reactor (position L-67) for either 24 (NM-104) or 100 hours (NM-107). Samples were loaded within and Al disc that was enclosed within an evacuated quartz vessel.

Fluence gradients were monitored with Fish Canyon (FC-2) sanidine. Typically fusing 4 crystals from each location monitored 4 to 6 locations within individual sample

trays. A sine curve was fit to the mean value of each location and J-factors were determined for the unknowns based on their geometry and the calculated curve. J-factor errors are estimated at 0.1 to 0.2% (1σ). Correction factors for interfering reactions were measured with K-glass and CaF_2. Typically 4 to 5 grains of each were fused with the CO_2 laser to obtain a weighted mean value for each correction factor.

Reported ages for step-heated samples are weighed by the inverse variance for the indicated steps. MSWD values are calculated for each weighted mean and errors are determined using the method of Taylor (1982). If the MSWD value is greater than 1, the error is multiplied by the square root of the MSWD. No strict plateau criteria were adhered to; rather weighted means were calculated for the flattest parts of each age spectrum. Total gas ages we determined by summing all of the isotopes for all steps and errors were calculated by quadradically summing individual errors from each heating step.

Monitor age and decay constants:

The assigned age of Fish Canyon sanidine is 27.84 Ma and the total ^{40}K decay constant is 5.543e-10/a. This value is relative to MMhb-1 hornblende at 520.4 Ma (Samson and Alexander, 1987; Denio and Potts, 1990).

References Cited:

Deino, A., and Potts, R., 1990. Single-Crystal $^{40}Ar/^{39}Ar$ dating of the Olorgesailie Formation, Southern Kenya Rift, J. Geophys. Res., 95, 8453-8470.

Samson, S.D., and E.C. Alexander, Jr., 1987, Calibration of the interlaboratory $^{40}Ar/^{39}Ar$ dating standard, Mmhb-1, Chem. Geol. Isot. Geosci., 66, 27-34.

Steiger, R.H. and Jager, E., 1977. Subcommission on geochronology: Convention on the use of decay constants in geo- and cosmochronology. Earth and Planet. Sci. Lett., 36: 359-362.

Taylor, J.R., 1982, An Introduction to Error Analysis: The Study of Uncertainties in Physical Measurements, Univ. Sci. Books, Mill Valley, Calif., 270 p.

K-feldspar argon data are presented in the context of the MDD model that is fully described in Appendix II. Each K-feldspar result is shown in a 4 panel plot as follows: a) measured spectrum (green) and model spectra (red); b) measured (black) and model (red) Arrhenius diagram with D/r^2 values determined using a slab geometry, c) $logr/r_o$ diagram with measured data presented in black and model data in red, and d) thermal histories that provided the model spectra when the thermal history is imposed upon the model kinetic parameters. In the thermal histories, the red and yellow bands represent the distribution of at least 20 models that assume only cooling from an initially high temperature where as the black lines represent thermal histories that allow for reheating. Because the reheating models significantly visually obscure the cooling only models for KGB99-32a, we have added a 5^{th} panel (e) for the this sample that separates the two thermal history scenarios. In the body of the manuscript we focus on samples KGB99-1, KGB99-27 and KGB99-32a and add into our models understanding of the geological information such as position relative to the Great Unconformity and relative structural position between samples. Because the models presented below are intended to be given with as few assumptions as possible they are not all necessarily consistent with geological relationships, but do represent the least biased view of the thermal history calculations.

In addition to the argon presentation in figure form, a complete table of isotopic data is also provided.

Information on samples dated by the $^{40}Ar/^{39}Ar$ method

Sample		Description	Location	Minerals dated
KGB99-1		Leuco-granite	Just beneath Tapeats at Azure Ridge	K-spar
KGB99-16		Paleoproterozoic granitiod	Pig's Ear	Hornblende, biotite, K-spar
KGB99-25		Pegmatite	Central-west side of block in ultramafic area	Muscovite
KGB99-27		Gold Butte Granite	E side of Garett Butte	Biotite, K-spar
KGB99-32a		Laramide pluton	West-side of block	Muscovite, biotite, K-spar
KGB99-34		Gold Butte Granite	West edge of pluton	Hornblende, biotite, K-spar

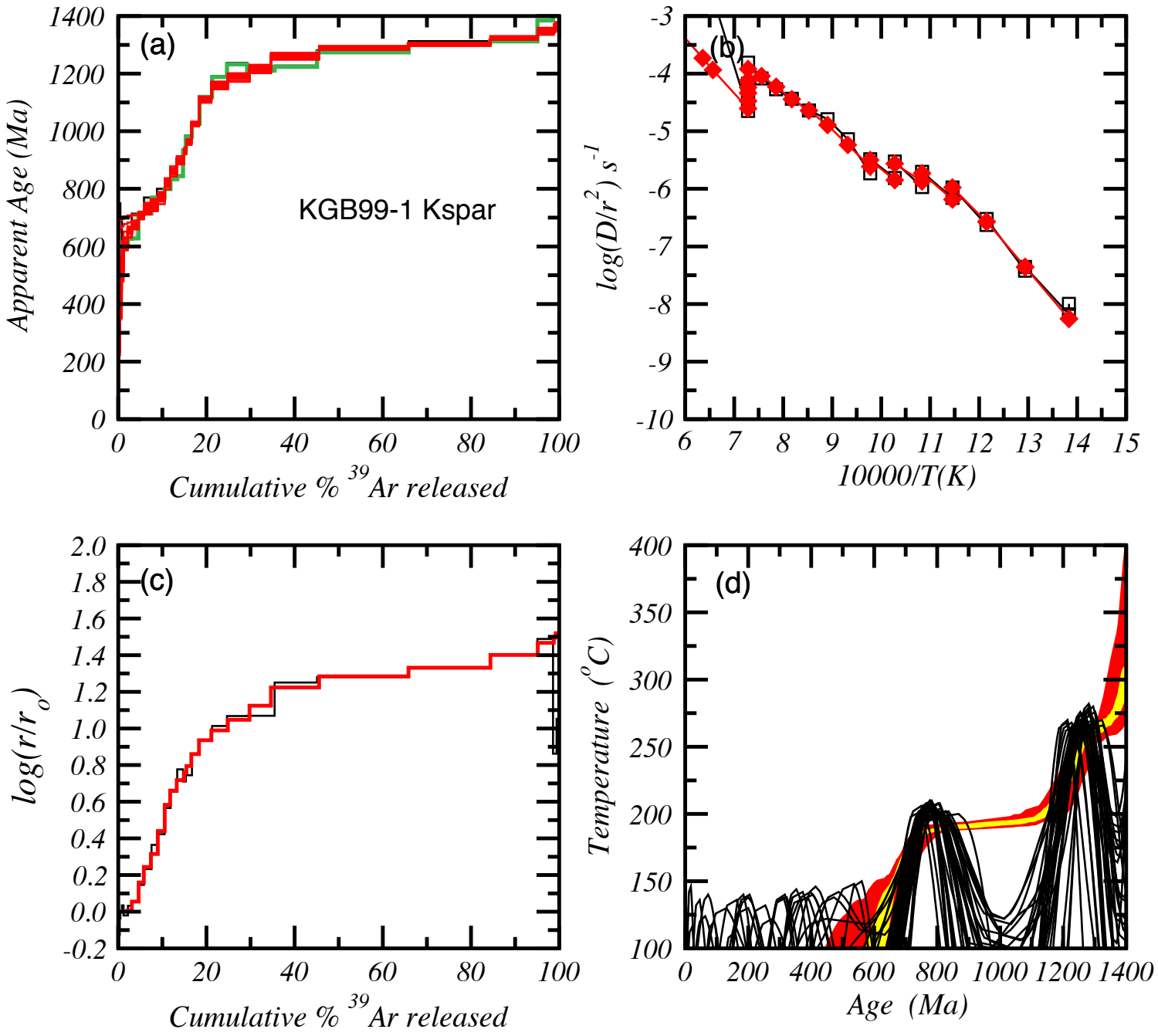

Fig. DR1. K- feldspar from KGB99-1, just beneath Tapeats Sandstone near Azure Ridge. a) measured spectrum (green) and model spectra (red); b) measured (black) and model (red) Arrhenius diagram with D/r2 values determined using a slab geometry, c) logr/ro diagram with measured data presented in black and model data in red, and d) thermal histories that provided the model spectra when the thermal history is imposed upon the model kinetic parameters; the red and yellow bands represent the distribution of at least 20 models that assume only cooling from an initially high temperature where as the black lines represent thermal histories that allow for reheating.

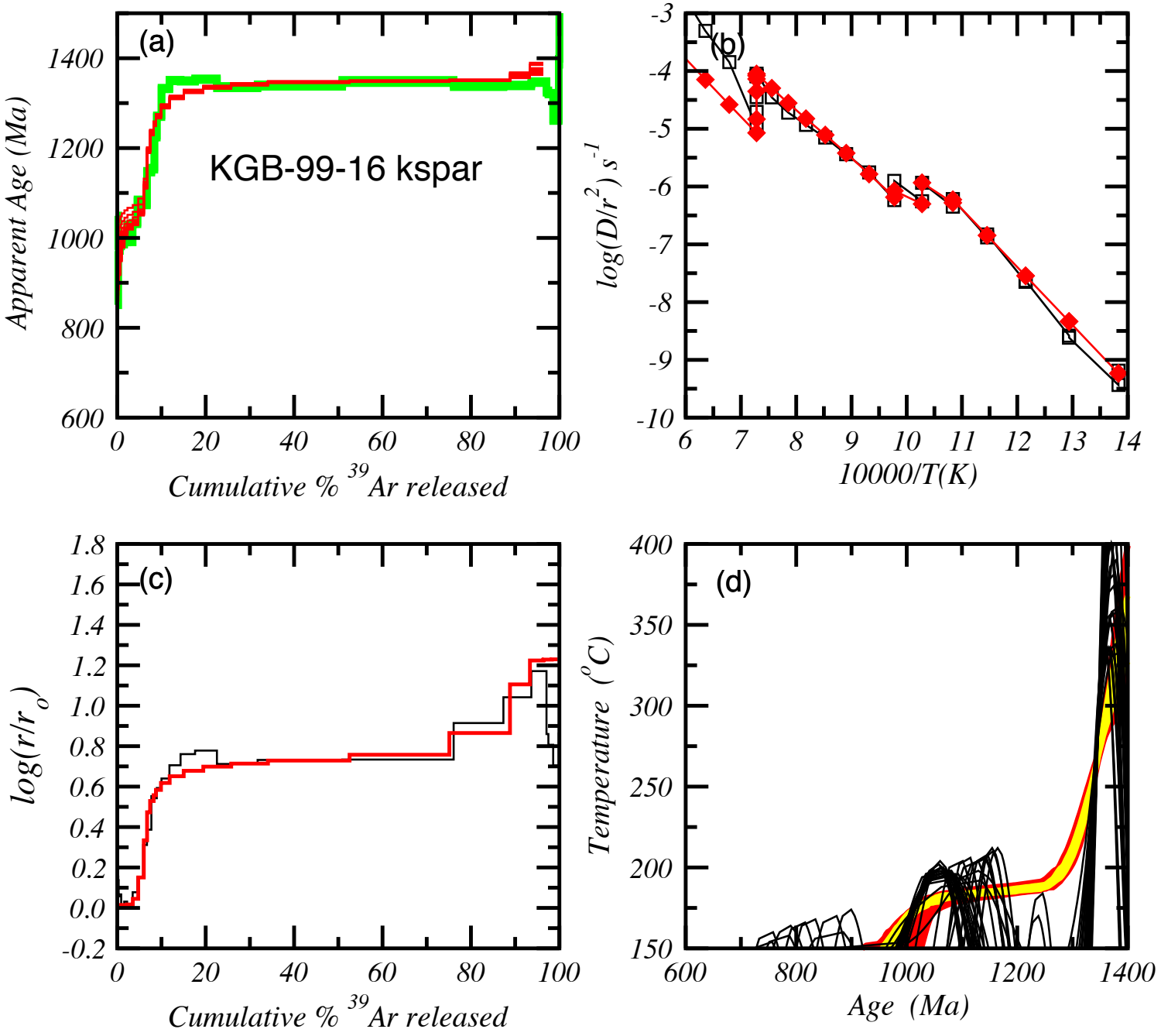

Fig. DR2. K- feldspar from KGB99-16, Paleoproterozoic granite from basement window north of Gold Butte fault. a) measured spectrum (green) and model spectra (red); b) measured (black) and model (red) Arrhenius diagram with D/r2 values determined using a slab geometry, c) logr/ro diagram with measured data presented in black and model data in red, and d) thermal histories that provided the model spectra when the thermal history is imposed upon the model kinetic parameters; the red and yellow bands represent the distribution of at least 20 models that assume only cooling from an initially high temperature where as the black lines represent thermal histories that allow for reheating.

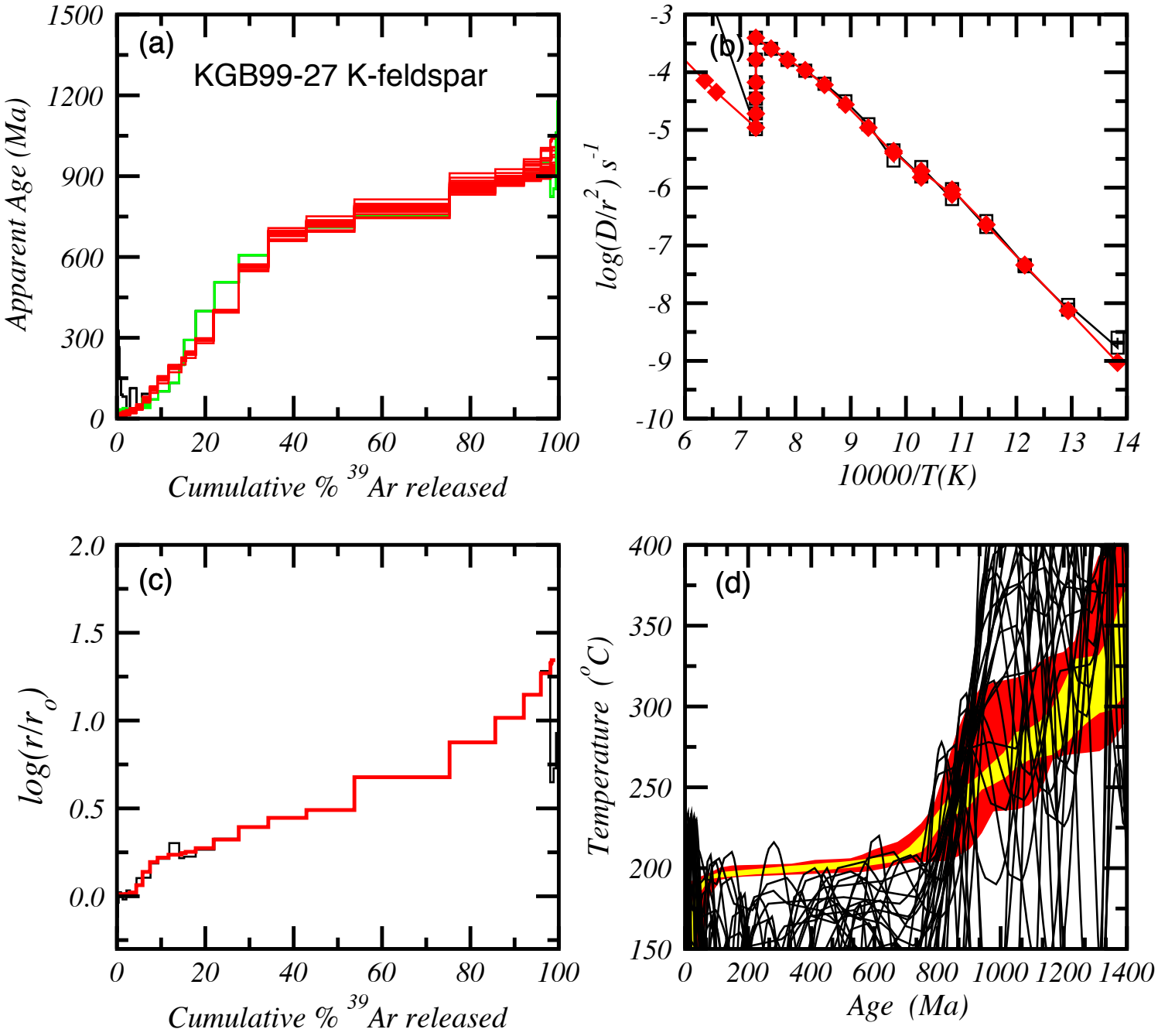

Fig. DR3. K- feldspar from KGB99-27, Gold Butte granite on east side of Garrett Butte. a) measured spectrum (green) and model spectra (red); b) measured (black) and model (red) Arrhenius diagram with D/r2 values determined using a slab geometry, c) logr/ro diagram with measured data presented in black and model data in red, and d) thermal histories that provided the model spectra when the thermal history is imposed upon the model kinetic parameters; the red and yellow bands represent the distribution of at least 20 models that assume only cooling from an initially high temperature where as the black lines represent thermal histories that allow for reheating.

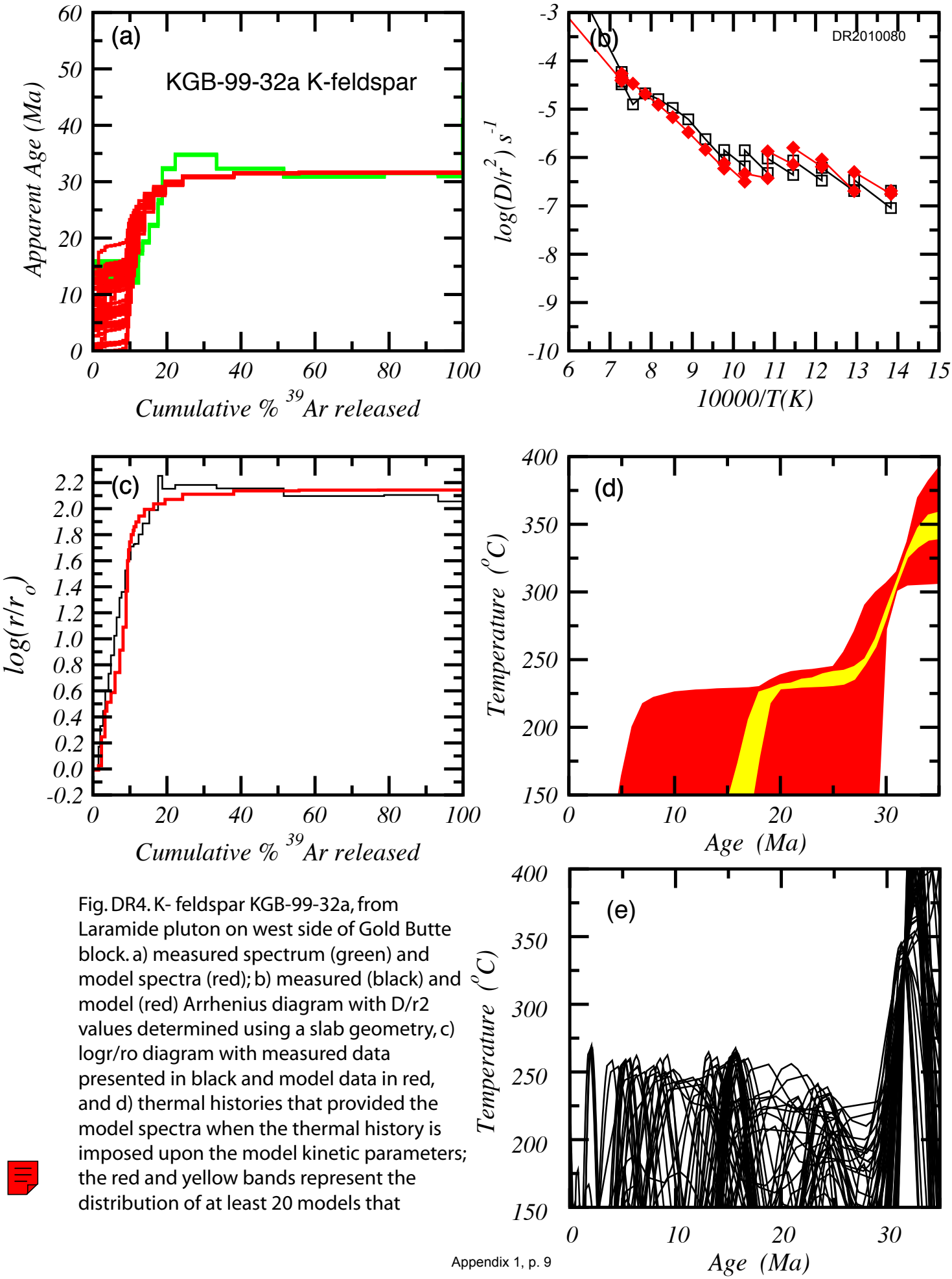

Fig. DR4. K- feldspar KGB-99-32a, from Laramide pluton on west side of Gold Butte block. a) measured spectrum (green) and model spectra (red); b) measured (black) and model (red) Arrhenius diagram with D/r2 values determined using a slab geometry, c) logr/ro diagram with measured data presented in black and model data in red, and d) thermal histories that provided the model spectra when the thermal history is imposed upon the model kinetic parameters; the red and yellow bands represent the distribution of at least 20 models that

	ID	Temp (°C)	$^{40}Ar/^{39}Ar$	$^{37}Ar/^{39}Ar$	$^{36}Ar/^{39}Ar$ (x 10^{-3})	$^{39}Ar_K$ (x 10^{-15} mol)	K/Ca	$^{40}Ar^*$ (%)	^{39}Ar (%)	Age (Ma)	±1σ (Ma)	Time (min)
	KGB-99-1 C:2:107, K-feldspar, 1.64 mg, J=0.0161952±0.10%, D=1.0024±0.001, NM-107, Lab#=50303-01											
x	A	450	323.0	0.0184	36.58	3.12	27.7	96.7	0.3	3249	5	14.3
x	B	450	36.96	0.0083	6.670	1.428	61.7	94.7	0.5	809.5	5.6	24.5
x	C	500	36.60	0.0100	3.942	3.37	51.0	96.8	0.8	817.7	2.6	14.1
x	D	500	25.16	0.0158	2.809	3.24	32.3	96.7	1.2	598.7	2.9	24.2
x	E	550	34.52	0.0109	1.429	9.47	46.7	98.8	2.2	792.8	1.5	14.8
x	F	550	25.98	0.0076	1.012	8.02	67.2	98.9	3.0	626.8	1.4	24.8
x	G	600	35.83	0.0070	1.003	14.50	72.4	99.2	4.6	819.6	1.4	14.6
x	H	600	30.14	0.0071	0.6254	11.84	71.9	99.4	5.8	713.0	1.1	24.7
x	I	650	35.08	0.0084	0.9273	15.89	60.4	99.2	7.5	806.0	1.3	15.0
x	J	650	33.00	0.0110	0.4976	11.81	46.3	99.6	8.8	769.1	1.1	25.0
x	K	700	36.42	0.0140	0.8883	16.40	36.3	99.3	10.5	831.1	1.2	14.8
x	L	700	34.55	0.0158	0.3688	12.43	32.4	99.7	11.8	799.1	1.3	25.1
x	M	750	36.45	0.0189	0.6166	14.43	26.9	99.5	13.4	833.2	1.2	15.5
x	N	750	37.05	0.0228	0.6210	12.16	22.3	99.5	14.7	844.1	1.4	25.5
x	O	800	42.06	0.0299	0.6404	6.09	17.1	99.6	15.3	933.5	1.8	3.5
x	P	850	45.27	0.0404	2.117	13.11	12.6	98.6	16.7	981.2	1.5	3.6
x	Q	900	47.63	0.0548	1.095	16.44	9.3	99.3	18.5	1025.8	1.6	3.5
x	R	950	53.32	0.0530	0.7968	26.6	9.6	99.6	21.3	1119.0	1.4	4.0
x	S	1000	57.76	0.0278	0.6292	31.7	18.4	99.7	24.7	1188.1	1.6	3.8
x	T	1050	60.76	0.0149	0.6586	43.0	34.1	99.7	29.2	1232.8	2.1	3.9
x	U	1100	59.31	0.0145	0.6728	58.7	35.2	99.7	35.5	1211.2	2.4	3.4
x	V	1100	60.14	0.0142	0.6398	90.6	35.8	99.7	45.1	1223.7	2.0	15.1
x	W	1100	63.68	0.0208	0.6010	195.7	24.5	99.7	65.9	1275.6	3.6	54.3
x	X	1100	65.81	0.0204	0.6434	173.6	25.1	99.7	84.3	1305.9	4.7	114.8
x	Y	1100	66.41	0.0198	0.9581	101.2	25.8	99.6	95.1	1313.0	3.2	235.9
x	Z	1100	71.93	0.0107	2.274	33.3	47.6	99.1	98.6	1384.0	1.5	377.6
x	ZA	1250	75.19	0.0097	0.6118	7.55	52.5	99.8	99.4	1434.1	2.2	2.7
x	ZB	1300	74.42	0.0377	1.068	3.19	13.5	99.6	99.7	1422.2	3.3	3.9
x	ZC	1400	79.52	0.0247	3.938	2.42	20.6	98.5	100.0	1477.9	4.8	4.3
x	ZE	1700	687.9	1.025	2272.4	0.074	0.50	2.4	100.0	426	99	2.4
	Integrated age ± 1σ		n=30			941.3		K2O=13.61%		1213.5	1.7	
	Plateau ± 1σ no plateau											
	KGB-99-16 D:1:107, Hornblende, 3.50 mg, J=0.0162518±0.10%, D=1.0024±0.001, NM-107, Lab#=50310-01											
x	A	800	23.00	0.7296	46.25	2.31	0.70	40.9	2.8	256.5	6.6	
x	B	900	79.33	0.4128	26.79	0.905	1.2	90.1	3.9	1390.4	9.5	
x	C	950	74.40	0.4450	6.090	0.486	1.1	97.6	4.5	1406.5	16.7	
x	D	1000	87.34	1.922	9.994	1.576	0.27	96.8	6.4	1561.2	6.0	
x	E	1050	87.62	2.212	5.044	2.93	0.23	98.5	9.9	1583.1	4.5	
x	F	1080	87.59	2.741	2.942	4.88	0.19	99.3	15.8	1591.3	3.0	
x	G	1100	87.12	2.843	2.329	5.09	0.18	99.5	22.0	1588.0	2.8	
x	H	1120	87.34	2.874	0.7737	5.76	0.18	100.0	29.0	1596.2	2.8	
	I	1140	88.72	3.135	1.164	22.7	0.16	99.9	56.4	1612.0	1.8	
x	J	1160	87.02	2.654	5.284	4.75	0.19	98.5	62.2	1575.7	3.2	
x	K	1180	87.10	2.673	6.497	3.38	0.19	98.1	66.3	1572.3	4.1	
	L	1220	88.72	3.588	0.8974	22.3	0.14	100.1	93.3	1613.7	2.1	
x	M	1300	88.84	3.428	5.683	4.45	0.15	98.5	98.7	1597.8	3.2	
x	N	1650	122.8	3.033	123.2	1.070	0.17	70.6	100.0	1588	12	
	Integrated age ± 1σ		n=14			82.6	0.17	K2O=0.56%		1571.2	1.7	
	Plateau ± 1σ steps I-L		n=2	MSWD=0.41		45.0			54.5	1612.7	1.7	

	ID	Temp (°C)	$^{40}Ar/^{39}Ar$	$^{37}Ar/^{39}Ar$	$^{36}Ar/^{39}Ar$ (x 10^{-3})	$^{39}Ar_K$ (x 10^{-15} mol)	K/Ca	$^{40}Ar^*$ (%)	^{39}Ar (%)	Age (Ma)	±1σ (Ma)	Time (min)
	KGB-99-16 C:11:107, Biotite, 0.71 mg, J=0.0160956±0.10%, D=1.0024±0.001, NM-107, Lab#=50309-01											
x	B	720	29.14	0.0488	36.51	3.26	10.5	63.0	1.2	466.6	6.6	
x	D	850	73.46	-0.0154	4.870	1.381	-	98.0	1.6	1388.3	6.0	
	E	900	74.27	0.0022	0.2209	29.7	232.3	99.9	12.2	1417.6	2.6	
	F	950	74.56	0.0059	0.4484	37.7	87.2	99.8	25.6	1420.5	2.3	
	G	1000	74.78	0.0061	0.4048	29.9	83.8	99.8	36.2	1423.5	1.9	
	H	1050	74.62	0.0062	0.2281	13.53	82.5	99.9	41.1	1422.2	1.8	
	I	1100	75.09	0.0185	0.2643	29.7	27.5	99.9	51.6	1428.2	1.6	
	J	1200	74.82	0.0323	0.3906	34.8	15.8	99.9	64.0	1424.2	1.9	
	K	1300	74.63	0.1150	0.2314	80.1	4.4	99.9	92.5	1422.4	2.6	
x	L	1650	78.42	0.0296	19.14	21.23	17.3	92.8	100.0	1398.4	2.4	
	Integrated age ± 1σ		n=10			281.4	11.8	K2O=9.46%		1412.0	1.6	
	Plateau ± 1σ steps E-K		n=7	MSWD=2.75		255.5			90.8	1423.6	1.6	
	KGB-99-16 C:10:107, K-feldspar, 2.05 mg, J=0.0160442±0.10%, D=1.00644±0.00091, NM-107, Lab#=50308-01											
x	A	450	358.3	0.1005	59.01	1.220	5.1	95.1	0.1	3368.4	9.6	25.0
x	B	450	83.47	0.2923	85.66	0.307	1.7	69.7	0.1	1189	26	25.0
x	C	500	61.64	0.4270	15.59	0.835	1.2	92.6	0.2	1172	11	14.6
x	D	500	55.09	0.4229	36.00	1.034	1.2	80.7	0.3	971.6	9.5	24.7
x	E	550	55.75	0.1006	7.707	3.25	5.1	95.9	0.6	1117.3	3.8	15.2
x	F	550	49.36	0.1813	13.76	3.15	2.8	91.8	0.9	985.2	4.0	25.2
x	G	600	49.56	0.1135	3.606	7.50	4.5	97.9	1.6	1038.0	3.0	14.9
x	H	600	46.54	0.0941	2.875	7.14	5.4	98.2	2.2	991.8	2.0	24.6
x	I	650	51.10	0.0416	0.6870	13.69	12.3	99.6	3.5	1076.6	1.6	15.4
x	J	650	48.63	0.0604	1.667	11.88	8.4	99.0	4.6	1032.1	1.7	25.4
x	K	700	51.55	0.1116	0.6794	14.21	4.6	99.6	5.9	1084.0	1.7	15.2
x	L	700	51.42	0.0471	2.341	9.37	10.8	98.7	6.7	1073.9	1.6	25.3
x	M	750	55.76	0.0732	1.150	10.91	7.0	99.4	7.7	1147.3	1.8	15.0
x	N	750	56.68	0.0939	2.798	7.65	5.4	98.6	8.4	1154.0	2.1	25.2
x	O	800	60.60	0.1415	-0.0805	5.86	3.6	100.1	8.9	1225.4	2.0	6.9
x	P	850	63.77	0.0811	0.0564	11.74	6.3	100.0	10.0	1270.8	1.9	7.3
x	Q	900	68.11	0.0597	-0.1378	19.50	8.5	100.1	11.8	1332.5	1.7	7.2
	R	950	69.45	0.0307	0.0562	27.8	16.6	100.0	14.3	1350.2	1.6	7.4
	S	1000	69.48	0.0734	0.3973	36.0	7.0	99.8	17.6	1349.3	1.6	7.2
	T	1050	69.73	0.0272	0.2569	54.0	18.8	99.9	22.5	1353.2	1.8	7.4
	U	1100	68.42	0.0447	0.1691	101.1	11.4	99.9	31.8	1335.6	2.6	7.3
	V	1100	68.73	0.0342	0.3480	209.8	14.9	99.9	50.9	1339.1	2.7	25.2
	W	1100	69.40	0.0283	0.3836	276.3	18.0	99.8	76.1	1348.2	3.7	59.9
	X	1100	68.86	0.0214	1.024	123.5	23.9	99.6	87.4	1338.2	2.5	121.8
	Y	1100	69.80	0.0217	3.943	69.1	23.5	98.3	93.7	1339.2	2.0	237.3
	Z	1100	73.44	0.0375	14.40	37.7	13.6	94.2	97.1	1346.8	2.2	486.8
x	ZA	1200	67.55	0.0999	-0.3251	4.55	5.1	100.2	97.5	1325.7	2.5	7.3
x	ZB	1300	67.49	0.0487	0.5548	11.98	10.5	99.8	98.6	1321.1	1.9	7.9
x	ZC	1400	63.33	0.0874	0.6815	13.72	5.8	99.7	99.9	1261.8	1.7	8.0
x	ZD	1500	74.58	0.4779	7.200	1.433	1.1	97.2	100.0	1391.9	6.4	7.9
x	ZE	1700	178.9	1.288	248.2	0.151	0.40	59.1	100.0	1790	52	7.4
	Integrated age ± 1σ		n=31			1096.4	12.6	K2O=12.80%		1323.9	1.7	
	Plateau ± 1σ steps R-Z		n=9	MSWD=8.67		935.3			85.3	1346.0	2.3	

	ID	Temp (°C)	$^{40}Ar/^{39}Ar$	$^{37}Ar/^{39}Ar$	$^{36}Ar/^{39}Ar$ (x 10^{-3})	$^{39}Ar_K$ (x 10^{-15} mol)	K/Ca	$^{40}Ar^*$ (%)	^{39}Ar (%)	Age (Ma)	±1σ (Ma)	Time (min)
	KGB-99-25:#2:107, 1.10 mg muscovite, J=0.0165±0.10%, D=1.0052±0.00121, NM-107, Lab#=50346-01											
x	A	600	93.08	0.0010	112.8	0.612	510.2	64.2	0.1	1238	10	
	B	650	69.51	0.0010	6.609	0.569	510.2	97.2	0.3	1350.6	6.2	
	C	700	70.67	0.0010	10.81	1.062	510.2	95.5	0.5	1349.6	4.7	
	D	750	70.87	0.0010	11.60	3.51	510.2	95.2	1.3	1349.1	2.5	
	E	800	70.71	0.0010	12.37	9.99	510.2	94.8	3.5	1343.6	2.1	
	F	840	67.47	0.0010	0.8971	96.2	510.2	99.6	24.9	1345.8	2.1	
	G	880	67.29	0.0010	0.1754	114.3	510.2	99.9	50.3	1346.2	2.6	
	H	920	67.20	0.0010	0.1781	67.6	510.2	99.9	65.4	1344.9	2.7	
	I	960	67.63	0.0010	0.5019	29.3	510.2	99.8	71.9	1349.6	2.0	
	J	1000	67.42	0.0010	1.068	14.59	510.2	99.5	75.1	1344.3	2.0	
	K	1040	67.40	0.0010	0.7438	15.6	510.2	99.7	78.6	1345.4	2.5	
	L	1080	67.72	0.0010	0.6318	17.3	510.2	99.7	82.5	1350.3	2.2	
	M	1120	67.60	0.0010	0.3929	30.6	510.2	99.8	89.3	1349.7	2.2	
	N	1160	67.29	0.0010	0.1312	40.8	510.2	99.9	98.3	1346.3	3.3	
	O	1200	67.65	0.0010	0.4904	4.12	510.2	99.8	99.2	1349.9	2.6	
	P	1250	67.88	0.0010	1.213	1.56	510.2	99.5	99.6	1350.2	4.0	
	Q	1350	67.08	0.0010	1.731	0.445	510.2	99.2	99.7	1336.7	9.9	
x	R	1650	68.81	0.0010	2.837	1.412	510.2	98.8	100.0	1356.5	3.9	
	Integrated age ± 1σ			n=18		449.6	510.2	K2O=9.52%		1346.4	1.7	
	Plateau ± 1σ	steps B-Q		n=16	MSWD=1.06	447.6			99.5	1347.2	1.1	

	ID	Temp (°C)	$^{40}Ar/^{39}Ar$	$^{37}Ar/^{39}Ar$	$^{36}Ar/^{39}Ar$ (x 10^{-3})	$^{39}Ar_K$ (x 10^{-15} mol)	K/Ca	$^{40}Ar^*$ (%)	^{39}Ar (%)	Age (Ma)	±1σ (Ma)	Time (min)
	KGB-99-27 D:7:107, K-feldspar, 1.87 mg, J=0.0160662±0.10%, D=1.0024±0.001, NM-107, Lab#=50314-01											
x	A	450	182.7	0.0100	30.07	1.86	50.9	95.1	0.2	2405.1	5.5	18.7
x	B	450	21.52	0.0033	10.25	0.696	156.1	85.9	0.3	468.6	7.0	24.7
x	C	500	13.43	0.0072	4.152	1.487	70.8	90.9	0.4	322.4	4.0	14.3
x	D	500	10.49	0.0060	2.559	1.452	84.5	92.8	0.6	261.5	3.7	24.4
x	E	550	5.783	0.0034	1.223	3.34	148.2	93.7	0.9	150.0	1.9	14.9
x	F	550	3.579	0.0008	1.454	3.86	656.2	87.9	1.3	88.3	1.5	25.0
x	G	600	3.145	0.0031	0.8358	8.44	165.3	92.1	2.2	81.35	0.80	14.7
x	H	600	1.454	0.0021	0.5801	7.62	240.7	88.0	2.9	36.03	0.70	24.8
x	I	650	4.299	0.0032	0.9231	14.56	158.0	93.6	4.4	112.35	0.52	15.1
x	J	650	1.493	0.0035	0.3371	11.89	147.5	93.2	5.6	39.18	0.46	25.1
x	K	700	3.365	0.0043	0.3151	19.4	118.5	97.2	7.6	91.69	0.38	15.0
x	L	700	2.630	0.0050	0.3357	17.3	101.1	96.2	9.4	71.16	0.44	25.0
x	M	750	3.662	0.0058	0.1873	24.3	88.2	98.5	11.9	100.88	0.29	15.5
x	N	750	4.800	0.0063	0.1418	21.8	81.0	99.1	14.1	132.17	0.34	25.6
x	O	800	7.347	0.0080	0.1944	10.92	63.8	99.2	15.2	199.10	0.68	3.4
x	P	850	11.03	0.0109	0.3344	25.7	46.6	99.1	17.8	291.26	0.44	3.6
x	Q	900	15.43	0.0110	0.1046	41.5	46.4	99.8	22.0	398.26	0.59	3.5
x	R	950	20.20	0.0093	0.1647	54.5	54.6	99.8	27.6	505.45	0.82	3.4
x	S	1000	24.91	0.0066	0.1611	65.3	77.3	99.8	34.3	605.70	0.95	3.3
x	T	1050	27.64	0.0050	0.1698	84.0	102.9	99.8	42.8	661.48	0.93	3.4
x	U	1100	30.07	0.0052	0.1356	107.2	98.1	99.9	53.8	709.7	1.1	3.5
x	V	1100	32.37	0.0049	0.1809	210.7	103.2	99.8	75.3	753.9	1.3	25.4
x	W	1100	37.10	0.0039	0.2509	101.5	131.4	99.8	85.6	841.5	1.5	54.7
x	X	1100	39.55	0.0023	0.3333	63.1	217.7	99.8	92.1	885.1	1.3	114.7
x	Y	1100	40.96	0.0020	0.7779	38.3	254.4	99.4	96.0	907.7	1.5	234.7
x	Z	1100	43.81	0.0022	3.032	20.5	230.8	98.0	98.0	945.6	1.4	474.7
x	ZA	1250	36.13	0.0005	0.3672	7.61	1108	99.7	98.8	823.4	1.4	3.4
x	ZB	1300	37.67	-0.0001	0.3006	5.34	-	99.8	99.4	851.7	1.4	3.7
x	ZC	1400	50.15	0.0029	1.548	2.88	177.1	99.1	99.7	1058.4	2.3	3.9
x	ZD	1700	60.51	0.0035	11.90	3.34	146.4	94.2	100.0	1172.3	2.8	3.6
	Integrated age ± 1σ		n=30			980.3	98.0	K2O=12.53%		647.33	0.84	
	Plateau ± 1σ no plateau											
	KGB-99-27 D:5:107, Biotite, 0.71 mg, J=0.0161481±0.10%, D=1.0024±0.001, NM-107, Lab#=50313-01											
x	A	650	38.88	0.0222	73.49	16.5	22.9	44.1	7.5	440.9	3.2	
x	B	720	43.28	0.0153	7.097	17.4	33.3	95.2	15.3	919.4	1.5	
x	C	800	52.72	0.0119	2.284	13.61	42.9	98.7	21.5	1100.3	1.4	
x	D	850	57.77	0.0095	0.7202	28.7	53.8	99.6	34.5	1185.4	1.3	
x	E	900	60.68	0.0094	0.4954	23.9	54.3	99.8	45.4	1229.9	1.5	
x	F	950	62.21	0.0118	0.3773	19.2	43.2	99.8	54.0	1252.8	1.5	
x	G	1000	62.01	0.0150	0.3910	16.5	34.1	99.8	61.5	1249.7	1.5	
x	H	1050	61.47	0.0117	0.3636	18.8	43.7	99.8	70.1	1242.0	1.6	
x	I	1100	61.42	0.0111	0.3953	22.0	46.1	99.8	80.0	1241.1	1.6	
x	J	1200	60.07	0.0144	0.9324	22.9	35.5	99.6	90.4	1218.9	1.5	
x	K	1300	63.27	0.2130	0.9918	21.2	2.4	99.6	100.0	1265.8	1.6	
	Integrated age ± 1σ		n=11			220.7	15.9	K2O=7.39%		1152.6	1.3	
	Plateau ± 1σ no plateau											

	ID	Temp (°C)	$^{40}Ar/^{39}Ar$	$^{37}Ar/^{39}Ar$	$^{36}Ar/^{39}Ar$ (x 10^{-3})	$^{39}Ar_K$ (x 10^{-15} mol)	K/Ca	$^{40}Ar^*$ (%)	^{39}Ar (%)	Age (Ma)	±1σ (Ma)	Time (min)
	KGB9932A D:10:104, K-feldspar, 1.34 mg, J=0.0032888±0.10%, D=1.0024±0.001, NM-104, Lab#=50206-01											
x	A	450	27.12	0.0043	53.29	2.80	118.2	41.9	1.5	66.11	0.84	14.5
x	B	450	10.22	-0.0018	25.17	0.85	-	27.0	2.0	16.3	1.2	23.1
x	C	500	7.116	-0.0033	14.46	1.42	-	39.7	2.7	16.65	0.61	13.7
x	D	500	12.29	-0.0014	34.75	1.14	-	16.2	3.3	11.78	0.94	24.1
x	E	550	8.847	-0.0028	21.44	1.57	-	28.2	4.2	14.69	0.75	13.7
x	F	550	15.23	-0.0011	44.20	1.24	-	14.1	4.9	12.7	1.0	23.9
x	G	600	10.70	0.0002	27.46	1.64	2863	24.0	5.7	15.15	0.77	14.2
x	H	600	19.05	0.0004	60.86	1.22	1188	5.5	6.4	6.2	1.2	24.1
x	I	650	16.43	-0.0013	45.62	1.40	-	17.8	7.2	17.3	1.0	14.0
x	J	650	25.51	0.0004	78.98	1.08	1180	8.4	7.7	12.7	1.9	23.9
x	K	700	14.66	-0.0005	40.92	1.77	-	17.4	8.7	15.03	0.84	14.6
x	L	700	24.80	-0.0049	78.69	1.28	-	6.2	9.4	9.0	1.5	24.9
x	M	750	16.42	-0.0036	48.64	1.51	-	12.3	10.2	12.0	1.3	14.6
x	N	750	24.49	0.0001	76.15	1.49	4335	8.0	11.0	11.6	1.6	24.8
x	O	800	17.90	-0.0081	54.43	0.712	-	10.0	11.4	10.6	1.4	4.7
x	P	850	10.04	-0.0023	26.10	1.73	-	23.0	12.3	13.58	0.76	4.7
x	Q	900	3.471	0.0011	1.689	2.04	470.2	85.5	13.4	17.41	0.32	3.5
x	R	950	3.783	-0.0004	1.687	3.34	-	86.7	15.2	19.24	0.21	4.2
x	S	1000	4.380	0.0020	2.018	4.39	255.7	86.3	17.6	22.16	0.18	4.8
x	T	1050	5.333	0.0002	2.824	2.10	3219	84.3	18.7	26.35	0.38	4.3
x	U	1100	6.596	0.0033	3.730	6.46	154.9	83.2	22.2	32.16	0.17	5.0
x	V	1100	6.848	0.0040	3.148	20.7	126.8	86.4	33.4	34.63	0.13	24.9
x	W	1100	6.237	0.0016	2.504	33.6	311.3	88.1	51.5	32.179	0.092	54.5
x	X	1100	5.941	0.0009	2.341	50.3	552.8	88.3	78.7	30.737	0.074	114.4
x	Y	1100	6.126	0.0008	2.579	27.0	647.1	87.5	93.3	31.401	0.100	166.8
x	Z	1100	7.726	0.0010	8.332	12.3	522.4	68.0	99.9	30.82	0.17	474.0
x	ZD	1400	10.97	-0.0240	11.70	0.204	-	68.4	100.0	43.9	3.1	5.5
	Integrated age ± 1σ		n=27			185.4	428.8	K2O=16.16%		29.64	0.10	
	Plateau ± 1σ no plateau											
	KGB9932a G:1:104, muscovite, 3 1mm flakes, 0.6 mg, J=0.0032588±0.10%, D=1.0024±0.001, NM-104, Lab#=50215-01											
x	AA	700	65.87	-0.0588	200.8	0.116	-	9.9	0.3	37.9	7.5	
x	B	800	25.17	0.0454	51.71	0.525	11.2	39.2	1.5	57.1	2.0	
x	C	900	17.49	-0.0016	23.40	2.78	-	60.4	8.1	60.98	0.62	
x	D	950	14.64	0.0007	9.808	3.52	688.6	80.2	16.4	67.58	0.39	
x	E	1000	12.32	0.0007	1.964	12.8	774.6	95.3	46.5	67.59	0.14	
x	F	1050	12.20	0.0046	2.847	2.79	109.7	93.1	53.1	65.43	0.30	
x	G	1100	12.82	0.0000	3.990	2.44	10286	90.8	58.9	67.01	0.31	
x	H	1150	12.69	0.0006	3.136	4.87	837.4	92.7	70.4	67.70	0.20	
x	I	1200	12.15	0.0001	0.9410	10.4	4248	97.7	94.8	68.34	0.13	
x	J	1250	12.75	-0.0035	2.091	1.46	-	95.1	98.2	69.79	0.41	
x	K	1300	15.71	-0.0195	8.724	0.199	-	83.6	98.7	75.5	2.0	
x	L	1700	16.36	-0.0040	14.07	0.549	-	74.5	100.0	70.2	1.3	
	Integrated age ± 1σ		n=12			42.4	727.5	K2O=8.32%		67.11	0.15	
	Plateau ± 1σ no plateau											

	ID	Temp (°C)	$^{40}Ar/^{39}Ar$	$^{37}Ar/^{39}Ar$	$^{36}Ar/^{39}Ar$ (x 10^{-3})	$^{39}Ar_K$ (x 10^{-15} mol)	K/Ca	$^{40}Ar^*$ (%)	^{39}Ar (%)	Age (Ma)	±1σ (Ma)	Time (min)
	KGB9932a D:11:104, biotite, 10 flakes, about 0.2 mm, 1.5 mg, J=0.0032895±0.10%, D=1.0024±0.001, NM-104, Lab#=50207-01											
	A	700	19.24	0.0271	36.97	4.67	18.8	43.2	5.7	48.54	0.51	
	B	800	8.540	0.0090	2.356	16.1	56.5	91.8	25.3	45.82	0.12	
	C	900	8.770	0.0022	1.452	15.1	226.8	95.1	43.7	48.69	0.11	
	D	950	8.933	0.0044	2.157	4.78	115.5	92.8	49.6	48.43	0.19	
	E	1000	9.071	0.0048	3.928	3.72	105.5	87.2	54.1	46.20	0.27	
	F	1050	8.787	0.0044	3.396	5.85	115.6	88.6	61.2	45.47	0.25	
	G	1100	8.733	0.0020	1.704	13.5	261.5	94.2	77.7	48.05	0.10	
	H	1150	8.938	0.0022	1.632	8.1	227.8	94.6	87.6	49.35	0.15	
	I	1200	9.106	0.0017	2.140	3.88	306.7	93.0	92.3	49.46	0.25	
	J	1250	9.218	0.0018	1.494	3.79	290.7	95.2	97.0	51.21	0.23	
	K	1300	9.721	0.0035	2.147	1.61	144.4	93.5	98.9	52.99	0.41	
	L	1700	17.96	0.0031	31.75	0.89	162.8	47.7	100.0	50.1	1.1	
	Integrated age ± 1σ			n=12		82.0	95.8	K2O=6.38%		47.97	0.11	
	Plateau ± 1σ	steps A-L		n=12	MSWD=89.38	81.998	171.880±92.80		100.0	48.08	0.48	
	KGB-99-34 E:1:107, K-feldspar, 1.92 mg, J=0.016±0.10%, D=1.0024±0.001, NM-107, Lab#=50318-01											
x	A	450	898.7	0.0573	46.52	0.720	8.9	98.5	0.1	4905	14	18.6
x	B	450	109.8	-0.0255	19.76	0.270	-	94.7	0.1	1767	16	24.6
x	C	500	70.39	0.0079	7.904	0.593	64.3	96.7	0.2	1328.6	8.1	14.3
x	D	500	97.46	0.0230	5.975	0.565	22.2	98.2	0.2	1675.1	9.1	24.4
x	E	550	54.02	0.0211	4.941	1.323	24.2	97.3	0.4	1100.7	3.9	14.9
x	F	550	7.805	0.0106	0.9939	1.079	47.9	96.2	0.5	204.1	4.3	25.0
x	G	600	14.26	0.0183	1.258	2.77	27.9	97.4	0.8	361.3	2.3	14.6
x	H	600	2.243	0.0210	1.570	2.57	24.3	79.1	1.0	49.9	2.0	24.8
x	I	650	24.20	0.0197	1.181	6.96	25.8	98.6	1.7	582.6	1.3	15.1
x	J	650	2.231	0.0164	0.7011	4.47	31.1	90.7	2.2	56.8	1.3	25.1
x	K	700	8.723	0.0229	0.4934	10.70	22.2	98.3	3.3	231.35	0.70	14.9
x	L	700	2.573	0.0199	0.2765	8.57	25.6	96.9	4.2	69.80	0.72	25.0
x	M	750	8.172	0.0253	0.5671	17.1	20.2	98.0	6.0	216.77	0.49	15.5
x	N	750	2.996	0.0269	0.4130	13.12	19.0	96.0	7.3	80.42	0.51	25.5
x	O	800	13.25	0.0310	0.8395	6.43	16.5	98.1	8.0	340.5	1.0	3.7
x	P	850	10.61	0.0310	0.2700	12.18	16.4	99.3	9.2	280.34	0.60	4.0
x	Q	900	22.29	0.0312	0.5868	15.7	16.4	99.2	10.9	546.12	0.77	4.1
x	R	950	37.37	0.0231	0.5452	15.6	22.1	99.6	12.5	842.2	1.0	3.5
x	S	1000	45.83	0.0165	0.8096	18.7	30.9	99.5	14.4	987.8	1.2	3.4
x	T	1050	43.97	0.0139	0.6118	26.3	36.7	99.6	17.1	957.5	1.3	3.5
x	U	1100	52.91	0.0120	0.8659	24.9	42.4	99.5	19.7	1102.1	1.5	3.3
x	V	1100	31.68	0.0114	0.6106	80.0	44.7	99.4	27.9	735.9	1.0	25.3
x	W	1100	25.62	0.0086	0.4152	100.6	59.6	99.5	38.3	616.80	0.90	54.8
x	X	1100	24.04	0.0086	0.4333	128.5	59.2	99.5	51.6	583.82	0.88	114.8
x	Y	1100	22.21	0.0070	0.5209	125.6	73.1	99.3	64.6	544.76	0.64	234.8
x	Z	1100	25.49	0.0067	0.9177	63.4	76.0	98.9	71.1	610.9	1.1	325.8
x	ZA	1250	20.76	0.0075	0.4345	66.7	68.4	99.4	78.0	513.96	0.98	3.9
x	ZB	1300	18.75	0.0070	0.4475	75.9	72.8	99.3	85.8	469.8	1.1	3.7
x	ZC	1400	22.19	0.0057	0.5724	53.2	89.0	99.2	91.3	544.03	0.92	4.2
x	ZD	1700	21.94	0.0070	0.7669	84.2	72.5	99.0	100.0	537.34	0.97	3.5
	Integrated age ± 1σ			n=30		968.7	48.8	K2O=12.11%		604.27	0.77	
	Plateau ± 1σ	no plateau										

	ID	Temp (°C)	$^{40}Ar/^{39}Ar$	$^{37}Ar/^{39}Ar$	$^{36}Ar/^{39}Ar$ (x 10^{-3})	$^{39}Ar_K$ (x 10^{-15} mol)	K/Ca	$^{40}Ar^*$ (%)	^{39}Ar (%)	Age (Ma)	±1σ (Ma)	Time (min)
	KGB-99-34 E:2:107, Hornblende, 2.80 mg, J=0.01628±0.10%, D=1.0024±0.001, NM-107, Lab#=50319-01											
x	A	800	71.95	1.197	64.56	1.469	0.43	73.6	1.1	1122.2	8.0	
x	B	900	45.27	0.8519	26.18	0.766	0.60	83.1	1.7	861.7	9.6	
x	C	950	40.42	1.146	5.478	0.530	0.45	96.2	2.1	885.3	13.7	
x	D	1000	54.32	1.881	4.881	1.391	0.27	97.7	3.1	1123.8	5.6	
x	E	1050	62.70	2.671	1.943	3.30	0.19	99.5	5.6	1265.6	3.0	
x	F	1080	68.12	3.155	2.590	5.63	0.16	99.3	9.8	1341.1	2.4	
x	G	1100	70.02	3.458	1.353	7.53	0.15	99.9	15.5	1373.2	2.3	
x	H	1120	72.34	3.471	1.164	3.66	0.15	99.9	18.2	1405.6	2.4	
	I	1140	71.17	3.465	1.210	16.5	0.15	99.9	30.6	1389.4	2.2	
	J	1160	69.47	3.455	0.9593	31.4	0.15	100.0	54.1	1367.1	1.9	
	K	1180	69.22	3.483	1.360	16.1	0.15	99.9	66.2	1362.2	1.9	
	L	1220	69.84	3.717	1.277	38.7	0.14	99.9	95.2	1371.5	2.5	
	M	1300	72.05	4.896	4.321	6.38	0.10	98.8	100.0	1391.4	2.1	
	Integrated age ± 1σ			n=13		133.4	0.15	K2O=1.12%		1360.3	1.6	
	Plateau ± 1σ	steps I-M		n=5	MSWD=41.58	109.083			81.8	1375.43	6.142	
	KGB-99-34 E:4:107, Biotite, 1.19 mg, J=0.01623±0.10%, D=1.0024±0.001, NM-107, Lab#=50320-01											
x	A	650	30.63	0.0159	53.40	1.305	32.2	48.5	0.4	389.1	9.1	
x	B	720	25.43	0.0104	14.61	4.19	49.0	83.0	1.6	531.2	2.8	
x	C	800	26.90	0.0057	4.703	15.7	88.8	94.8	6.1	624.4	1.1	
x	D	850	32.04	0.0025	1.293	35.7	200.9	98.8	16.5	747.5	1.7	
x	E	900	45.58	0.0051	0.2408	37.8	100.0	99.9	27.4	997.5	1.5	
x	F	950	57.01	0.0048	0.0293	31.8	106.2	100.0	36.6	1181.4	2.6	
x	G	1000	56.21	0.0055	0.1589	28.3	92.0	99.9	44.8	1168.6	1.4	
x	H	1050	52.08	0.0060	-0.0867	18.5	84.9	100.1	50.2	1105.2	1.5	
x	I	1100	45.13	0.0138	0.2981	28.2	36.9	99.8	58.3	989.5	1.3	
x	J	1200	37.78	0.0142	0.3570	37.8	35.9	99.7	69.3	860.4	1.3	
x	K	1300	59.99	0.0495	0.3403	73.8	10.3	99.8	90.6	1224.9	2.3	
x	L	1650	66.01	0.0052	0.5627	32.5	97.5	99.8	100.0	1311.1	1.8	
	Integrated age ± 1σ			n=12		345.7	31.4	K2O=6.88%		1057.3	1.3	
	Plateau ± 1σ	no plateau		n=0								

Notes:

Isotopic ratios corrected for blank, radioactive decay, and mass discrimination, not corrected for interfering reactions.
Errors quoted for individual analyses include analytical error only, without interfering reaction or J uncertainties.
Integrated age calculated by summing isotopic measurements of all steps.
Integrated age error calculated by quadratically combining errors of isotopic measurements of all steps.
Plateau age is inverse-variance-weighted mean of selected steps.
Plateau age error is inverse-variance-weighted mean error (Taylor, 1982) times root MSWD where MSWD>1.
Plateau error is weighted error of Taylor (1982).
Decay constants and isotopic abundances after Steiger and Jäger (1977).
x preceding sample ID denotes analyses excluded from plateau age calculations.
- No dectable 37Ar.
Weight percent K_2O calculated from ^{39}Ar signal, sample weight, and instrument sensitivity.
Ages calculated relative to FC-2 Fish Canyon Tuff sanidine interlaboratory standard at 27.84 Ma
Decay Constant (LambdaK (total)) = 5.543e-10/a
Correction factors:

NM-104	$(^{39}Ar/^{37}Ar)_{Ca}$ = 0.0007 ± 5e-05	NM-107	$(^{39}Ar/^{37}Ar)_{Ca}$ = 0.0007 ± 5e-05
	$(^{36}Ar/^{37}Ar)_{Ca}$ = 0.00027 ± 1e-05		$(^{36}Ar/^{37}Ar)_{Ca}$ = 0.00027 ± 1e-05
	$(^{38}Ar/^{39}Ar)_{K}$ = 0.0125		$(^{38}Ar/^{39}Ar)_{K}$ = 0.0125
	$(^{40}Ar/^{39}Ar)_{K}$ = 0.025 ± 0.005		$(^{40}Ar/^{39}Ar)_{K}$ = 0.0275 ± 0.0004

APPENDIX 2

$^{40}Ar/^{39}Ar$ K-feldspar Thermochronology and Multiple Diffusion Domain (MDD) Theory

Introduction

This overview of $^{40}Ar/^{39}Ar$ K-feldspar thermochronology summarizes the theory and methodology of the Multiple Diffusion Domain (MDD) model with specific examples to illustrate the procedures used at the New Mexico Geochronology Research Laboratory (NMGRL). Geochronology relies on the accumulation of a radiogenic daughter isotope that is produced by the radioactive decay of a parent isotope. The parent to daughter ratio is combined with known decay constant(s) to calculate a date for a sample. The calculated date may be a meaningful geological age (i.e. time of an eruption, growth of a mineral, etc.) provided the sample is a closed system with no gain or loss of the parent or daughter isotopes. Thermochronology is based on the same basic principles of geochronology, but rather than a date being related to a specific event, thermochronological data records the time when a sample passes through a certain temperature (Dodson, 1973). This temperature is defined as the closure temperature and reflects the temperature when the sample effectively ceases to loose a daughter product by diffusion. There are many themochronometers amongst the variety of radioactive decay schemes and closure temperatures are highly variable (McDougall and Harrison, 1999). For the K-Ar system, hornblende appears to have the highest closure temperature of about 500°C (Harrison, 1981) followed by micas that range between about 300 and 400°C (Robins, 1974; Harrison et al., 1985; Hames and Bowring, 1994; Grove and Harrison, 1996). Homogeneous orthoclase was determined to have a closure temperature of about 300°C (Foland, 1974). Foland (1974) also suggested that microcline would have a lower closure temperature due to fine-scale mircotextures. Significant work throughout the past two decades has utilized and explored the argon systematics of K-feldspar (see McDougall and Harrison, 1999 for a review). There are probably many factors that contribute to argon loss in this microstructurally complex mineral and the overall utility of $^{40}Ar/^{39}Ar$ dating is still debated (e.g. Parsons et al., 1999; Lovera et al., 1997; 2002).

For $^{40}Ar/^{39}Ar$ K-feldspar thermochronology at the NMGRL, we adopt the MDD model of Lovera et al. (1989) to extract thermal histories from step-heating data. This method views K-feldspars as having a number of different size diffusion domains each of which has a different closure temperature typically between ~300 and 175°C. Diffusion domains are discrete areas of varying length and are assumed to be separated by boundaries that are maintained at zero argon concentration. Given sufficient time and temperatures near or in excess of the closure temperature of a particular domain, radiogenic argon will diffuse to the domain boundary and escape from the K-feldspar. Because argon loss in K-feldspars occurs in the temperature range equivalent to those found at mid- to shallow crustal levels, K-feldspar $^{40}Ar/^{39}Ar$ thermochronology is an useful method for understanding the thermal history of an important crustal region. In addition, the K-feldspar system is sensitive to moderate thermal perturbations and therefore can be used to determine the timing of episodic argon loss events related to, for instance, magmatism, geothermal activity or burial.

K-feldspar $^{40}Ar/^{39}Ar$ data and plots

Age spectrum diagrams

The thermal history recorded by a K-feldspar can be determined by combining the age spectrum data and the laboratory degassing behavior of ^{39}Ar. The age spectrum is a measurement of the natural radiogenic ^{40}Ar ($^{40}Ar^*$) concentration distribution within the sample, whereas the degassing of the reactor-produced ^{39}Ar during step-heating is a measure of the K-feldspar closure temperatures. Below we demonstrate the steps used to recover thermal histories from $^{40}Ar/^{39}Ar$ K-feldspar step heating data. The first step is to create the age spectrum by high-resolution (~45 steps) step heating (Fig. 1a). Heating schedules typically begin at 400°C and include three to four isothermal steps for many of the lower temperature settings (Fig. 1b). The isothermal steps serve two primary purposes. The first is to resolve excess ^{40}Ar that is common in most K-feldspars. The excess ^{40}Ar appears to be cited in thermally distinct reservoirs as the first isothermal step commonly records an anomalously old apparent age relative to the next isothermal steps

at a given temperature (Figs 1a, b). When the next higher isothermal temperature group is carried out the 1st step is once again anomalously old and is followed by younger apparent ages (Fig. 1b). This behavior is thought to be caused by decrepitation of fluid inclusions that contain excess ^{40}Ar (Harrison et al., 1993, 1994). After initial decrepitation caused by the first of the isothermal replicate steps, the age typically decreases and then rises more uniformally as the true distribution of $^{40}Ar^*$ is less disturbed by the fluid-inclusion hosted excess argon. Moving to the next highest temperature of isothermal replicates causes decrepitation of new fluid inclusions that again causes the apparent age to increase significantly (Fig. 1a, b).

Because MDD theory does not allow for excess argon contamination, the anomalously old steps need correction prior to modeling the age spectrum. Harrison et al. (1993) developed a method to correct for fluid inclusion hosted excess argon though the recognition that the old apparent ages were correlated to Cl that is monitored by measuring $^{38}Ar_{Cl}$. Using the Harrison et al. (1993) approach for many of the Precambrian samples analyzed at the NMGRL, yields Cl-corrected ages that are negative indicating that the Cl cannot all be correlated to excess argon and thus the method of Harrison et al. (1993) is generally not employed. Rather, it is assumed that when the apparent age reaches a minimum for a given set of isothermal heating steps the measured age accurately records the true $^{40}Ar^*$ distribution. To correct the anomalously old apparent ages that are given by the 1st isothermal step they are decreased to the mean value of the previous and following steps (Fig. 1b, c). This procedure results in a corrected age spectrum that only records an overall increasing spectrum and is the spectrum used for thermal history modeling.

Arrhenius diagrams

The second purpose of the isothermal steps is to evaluate whether the calculated diffusion coefficients for the initial heating steps on the Arrhenius diagram are approximately the same. An Arrhenius diagram is a plot of inverse temperature (1/T) and frequency-factor length scale parameter (D/r^2) for each heating step (Fig. 2a). The

frequency-factor length scale ratio is determined from the fraction of ^{39}Ar released and the duration of each heating step assuming a plane-sheet geometry (eqs. 1 and 2).

$$f=1-(8/\pi^2)\exp(-\pi^2 Dt/4r^2) \quad \text{for } 0.45\leq f\leq 1 \quad \text{eq. 1}$$

$$f=(2/((\pi^{1/2}))(Dt/r^2)^{1/2} \quad \text{for } 0\leq f\leq 0.60 \quad \text{eq. 2}$$

where D = diffusion coefficient; f = fraction ^{39}Ar released; r = diffusion half width; t = time at temperature.

The slope of the Arrhenius data is a function of the activation energy (E) of a sample, however with multiple diffusion domains contributing gas to each temperature step the true slope can be difficult to determine. Lovera et al. (1989) demonstrated that the initial heating steps could yield diffusion coefficients with a slope that accurately records the true E if the gas released is dominated by only one of the diffusion domains. Subequal diffusion coefficients for isothermal replicate heating steps indicates gas release that is dominated by a single domain (Fig. 2b – data segment 1), whereas significant decreases of the diffusion coefficient during replicate temperature steps indicates gas evolution from a mixture of different domain sizes (Fig. 2b – data segment 2). Because up to 4 replicate isothermal steps are typically used for these samples the overall slope of the initial segment of the Arrhenius plot is generally underestimated by linear regression of all of the diffusion coefficients (Fig. 2b – data segment 3). Therefore, we calculate the slope of line segments between the last isothermal step of a temperature group and the 1st isothermal step of the next highest temperature group (Fig 2b – data segment 4). The individual line segments that yield similar values are averaged to estimate the E for each sample. Typically, the first 3 to 5 line segments yield similar slopes that are averaged to estimate the E of the sample. For an Arrhenius diagram with Y-axis of $\log(D/r^2)$ and X-axis of 10000/T the E is given in kcal/mol via equation 3.

$$E = m*2.303*19.87 \quad \text{eq. 3}$$

where m is slope, 2.303 is a log versus natural log conversion and 19.87 is the gas constant.

Once the E is determined, a reference Arrhenius law (r_o) with this E is projected through the initial heating steps (Fig. 2a – data segment 5). Another characteristic of the Arrhenius plot is the several isothermal heating steps conducted at 1100°C (Fig. 2a – data segment 6). Typically a K-feldspar is heated at 1100°C for several steps that total about 8 hours to facilitate substantial degassing prior to incongruent melting. Stepping above 1100°C, where the sample begins to degas via melting, is readily recognized on the Arrhenius plot by a calculated diffusion coefficient that is anomalously high relative to the projection of the lower temperature diffusion coefficients (Fig. 2a – data segment 7).

Log(r/r_o) diagrams

Recall, as small diffusion domains are exhausted of argon during initial heating steps, the slope of the Arrhenius data decrease as larger domains begin to contribute more ^{39}Ar. This, coupled with the fact that each diffusion coefficient datum on the Arrhenius plot is graphically displayed with a symbol of equal size makes it is difficult to visualize the domain distribution of the sample. Also, the Arrhenius plot varies with heating schedule, thus making it a somewhat ineffective in representing the diffusion domain distribution. Therefore, Lovera et al. (1991) devised the log(r/r_o) plot as an alternative method of portraying the Arrhenius data (Fig. 3). This is a plot of the log of the deviation of the measured data from r_o versus cumulative %^{39}Ar released. Dividing the deviation by 2 yields the parameter log(r/r_o) that represents the change in domain size (r) necessary to depart from r_o. For a single domain sample there would be no variation between r_o and the measured data and thus the log(r/r_0) plot would be a horizontal line with value equal to zero. Log(r/r_o) values increase as the measured frequency factors fall below r_o on the Arrhenius diagram. A log(r/r_o) value of 1 indicates a relative increase in diffusion domain size of 10 whereas a value of 2 means a domain size that is 100 times larger than r_0. For the example given in Fig. 3, the log(r/r_o) values climb almost immediately from zero indicating that there is very little gas in the smallest diffusion domain and the overall flat

part near a value of 2 indicates that the largest diffusion domain is about 100 times larger than the reference value. The nondiffusive loss of ^{39}Ar that stems from sample melting is quite apparent on the $\log(r/r_o)$ plot as noted by a sudden drop of the $\log(r/r_o)$ value near 75% cumulative $\%^{39}Ar$ released.

Modeling kinetic parameters and thermal histories

Once the activation energy and the maximum value on the $\log(r/r_o)$ plot are determined, the domain distribution (i.e. volume fraction, number of domains, relative sizes) can be obtained by modeling the fraction of ^{39}Ar released relative to the heating schedule (Lovera et al., 1989; 1991). Lovera developed a set of automated routines for modeling both the ^{39}Ar fraction released and age spectrum data. We generally use these programs in a semi-automated manner by inputting our determined E and restricting the number of diffusion domains. The programs are modified from routines given in Press et al. (1992) and use a variational method to calculate a nonlinear-square fit approximation of the $\log(r/r_0)$ and age spectrum diagrams. For the case of the age spectrum modeling, the thermal histories are approximated with the Chebyshev polynomials with the best-fit Chebyshev coefficients being found with the Levenberg-Marquard methods. After the kinetic parameters are determined, the measured age spectrum is forward modeled by inputting thermal histories that yield calculated spectra that match the measured ages. There are two types of thermal histories calculated by the Lovera programs. For monotonic thermal histories, the sample is only allowed to cool from an initially high temperature, whereas for the unconstrained thermal histories the sample is allowed to undergo reheating (Figs. 4, 5a, b). Individual thermal histories are accepted when they yield a model spectrum that meets the fitting criteria relative to the measured spectrum (Quidelleur et al., 1997), The individual models are contoured and displayed in two separate fashions. For the monotonic thermal histories, 90% confidence intervals are calculated for the mean as well as the overall distribution and are shown as black and grey bans, respectively (Fig. 4). For the unconstrained models, bins of time-temperature space are assigned and then the number of thermal histories that pass through an individual bin is calculated. The contour shading represents various percentages of the

number of time-temperature paths that pass through individual bins relative to the total number of solutions. The background region represents a density of acceptable solutions that is less then 2% of the total number of solutions.

References

Harrison, T.M., Heizler, M.T., Lovera, O.M., 1993, *In vacuo* crushing experiments and K-feldspar thermochronometry. Earth. Planet. Sci. Lett., 117, 169-180.

Harrison, T.M., Heizler, M.T., Lovera O.M. and Wenji, C., 1994, A chlorine disinfectant for excess argon. Earth Planet. Sci. Lett., 123, 95-104.

Lovera, O.M., Richter, F.M., Harrison, T.M., 1989, $^{40}Ar/^{39}Ar$ thermochronology for slowly cooled samples having a distribution of domain sizes: Journal of Geophysical Research, v. 94, p. 17,917-17,935.

Lovera, O.M., Harrison, T.M., Richter, F.M., 1991, Diffusion domains determined by ^{39}Ar released during step heating, Journal of Geophysical Research, v. 96, p. 2057-2069.

Press, W. H., Teukolsky, S.A., Vetterling, W.T., Flannery, B.P., 1992, Numerical recipes in FORTRAN: the art of scientific computing, Cambridge University Press, 2nd ed., 963 p.

Quidelleur, X., Grove, M., Lovera, O.M., Harrison, T.M., Yin, A., 1997, Thermal evolution and slip history of the Renbu Zedong Thrust, southeastern Tibet: Journal of Geophysical Research, v. 102, n. B2, p. 2659-2679.

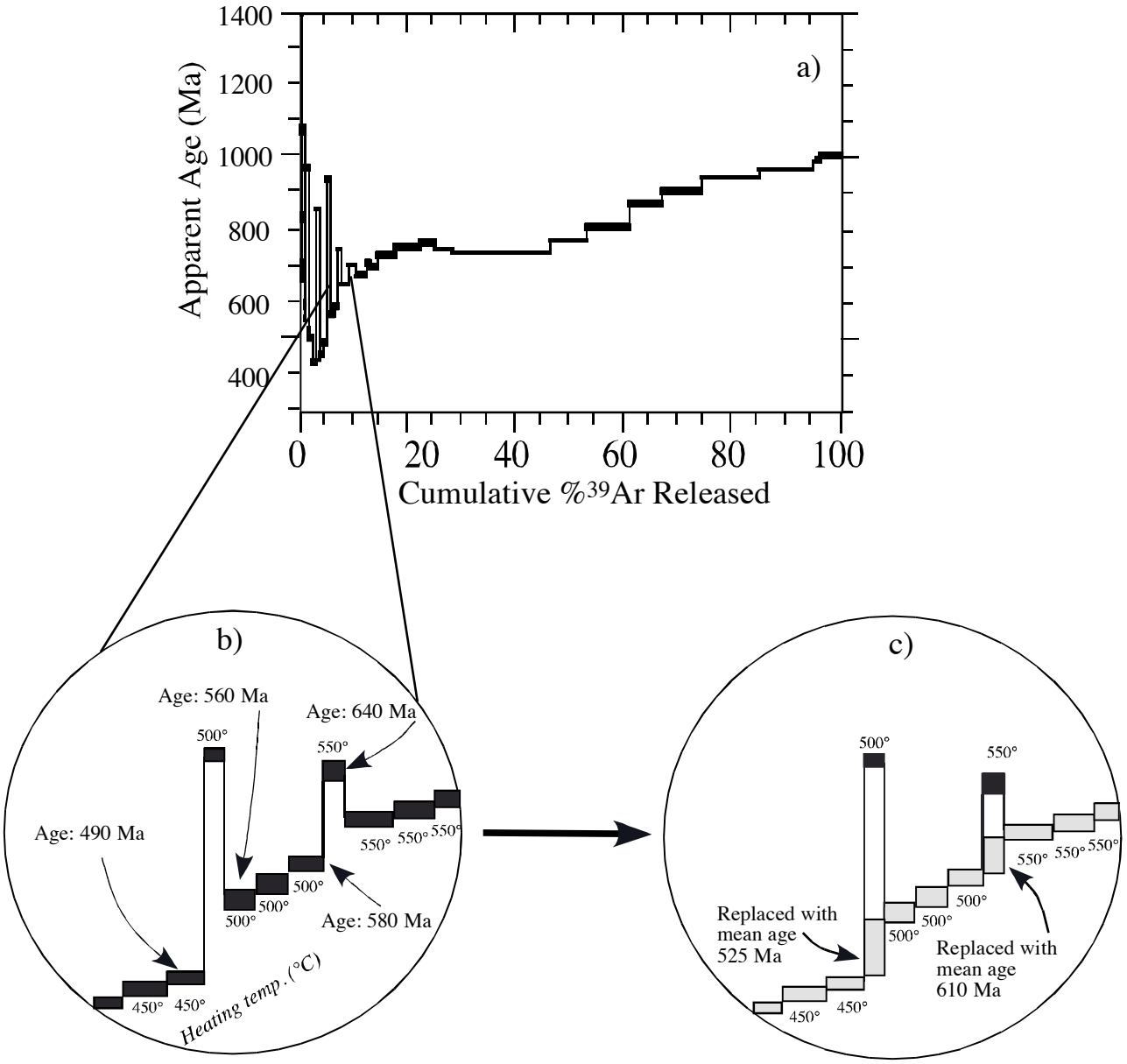

Fig. 1. Age spectrum diagram and excess argon corrections. 1a. Common age spectrum for many K-feldspars with initially old ages indicating excess ^{40}Ar contamination followed by an overall increasing age gradient revealing the non-uniform $^{40}Ar^*$ concentration profile developed by argon loss associated with slow-cooling and/or reheating events. 1b. Isothermal replicate heating steps demonstrate a characteristic behavior with the first step yielding an anomalously old age caused by degassing of fluid inclusions that host excess ^{40}Ar. 1c. Method of correcting anomalous ages involves substituting old ages with the mean age of the preceding and following steps. The error bar is expanded to fill the age space between the preceding and following steps.

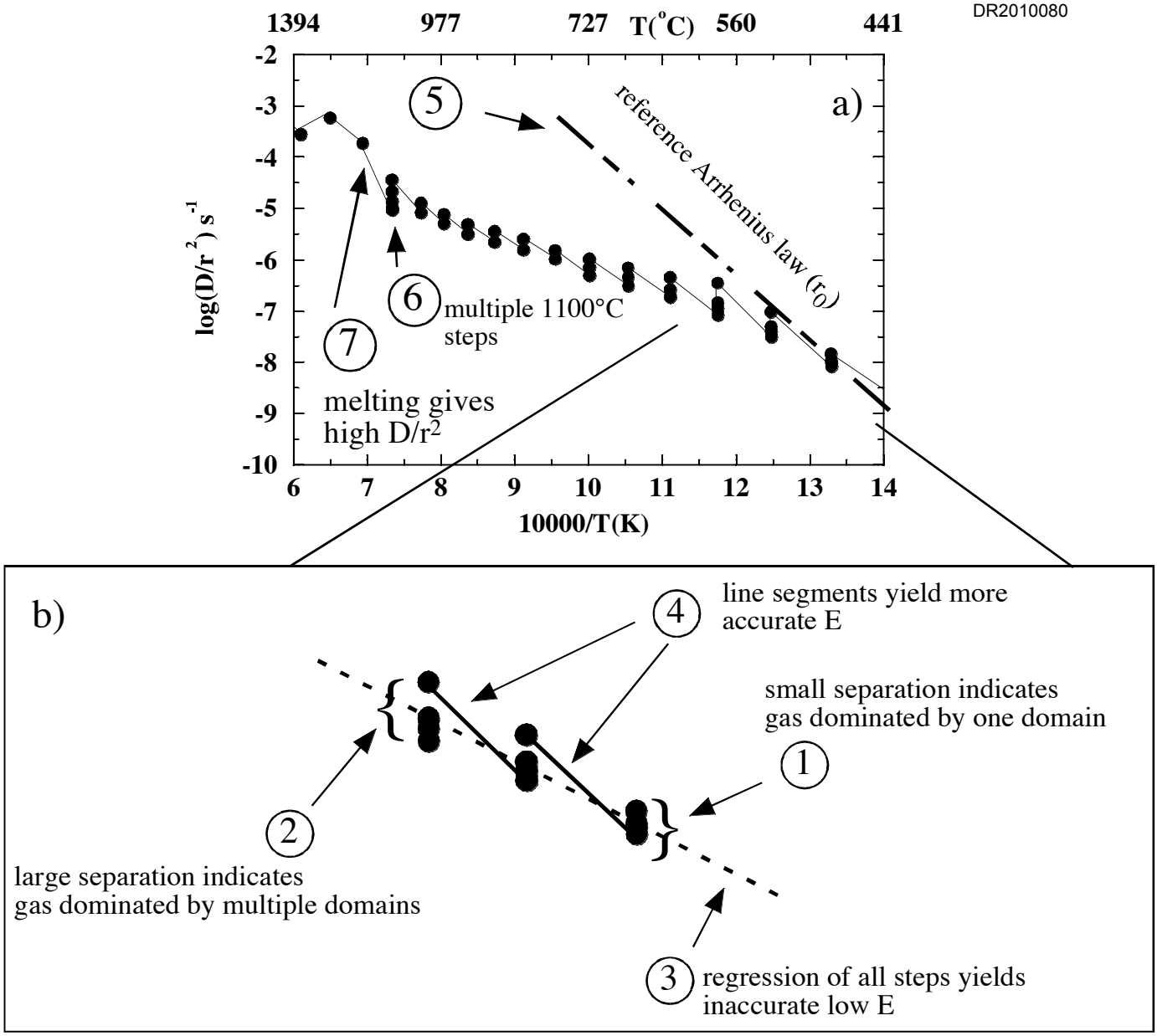

Fig. 2 Arrhenius diagram. 1a. Typical K-feldspar Arrhenius diagram for samples containing multiple diffusion domains. 1b. Expansion of initial part of the Arrhenius diagram to demonstrate characteristic data and choice of best E. 1, when isothermal steps yield similar $\log(D/r_2)$ values it is inferred that gas released is dominated by a single domain, whereas 2, shows significant decrease of $\log(D/r_2)$ values for isothermal steps that indicate a transition to degassing of larger diffusion domains. 3, regression of all initial data would provide an E that is underestimated due to ^{39}Ar derived from multiple domains. 4, line segments connecting last step of isothermal group with 1st step of next highest temperature isothermal group can be used to better determine the slope (E) of r_o. 5, by convention the reference Arrhenius law is projected through initial heating steps such that the initial steps on $\log(r/r_o)$ are zero. 6, several steps at 1100°C are carried out to degas the sample prior to the onset of melting. 7, once the temperature is raised above 1100°C high apparent $\log(D/r^2)$ values are calculated due to enhanced argon loss via melting compared to diffusive argon loss. Data collected above 1100°C are not used for modeling since the argon loss from the sample is not occurring by the same mechanism that occurred in nature.

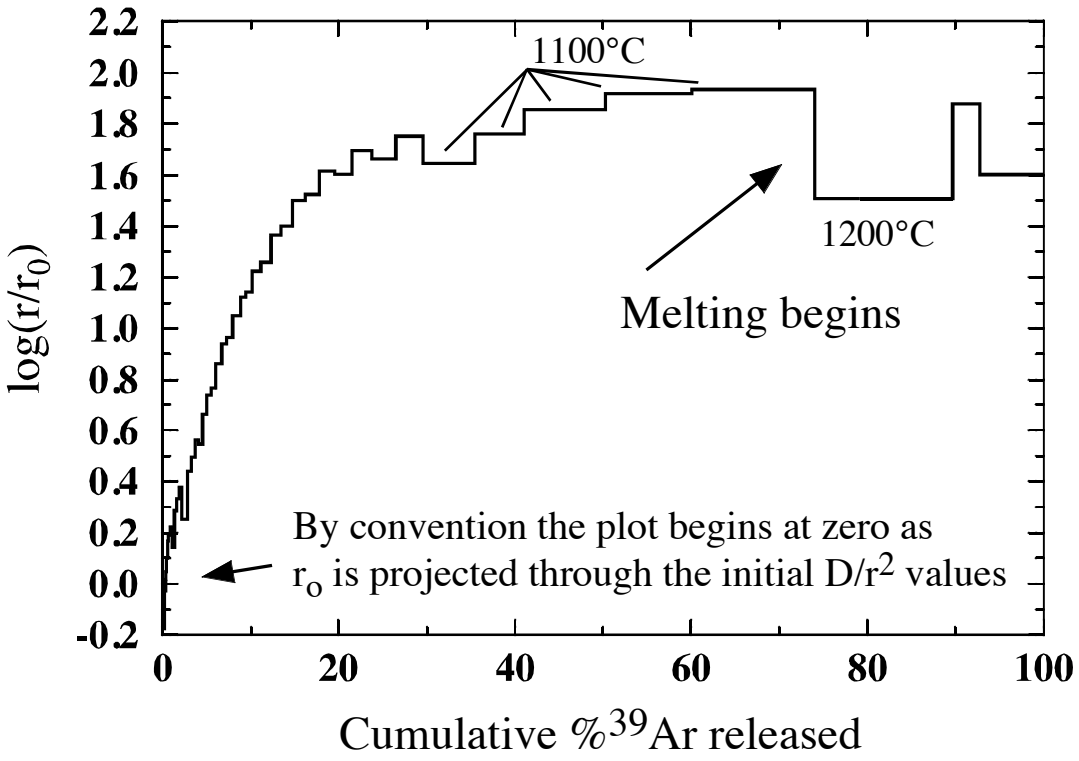

Fig. 3. Log(r/r_o) diagram. This plot is intended to provide a method to show how much ^{39}Ar is contained in an individual point on the Arrhenius plot. The log(r/r_o) value represents the relative domain size compared to r_o that has caused deviation from the reference Arrhenius law. A value of 1 indicates that r is 10 times larger than r_0 whereas a value of 2 indicates that r is 100 times larger than r_o.

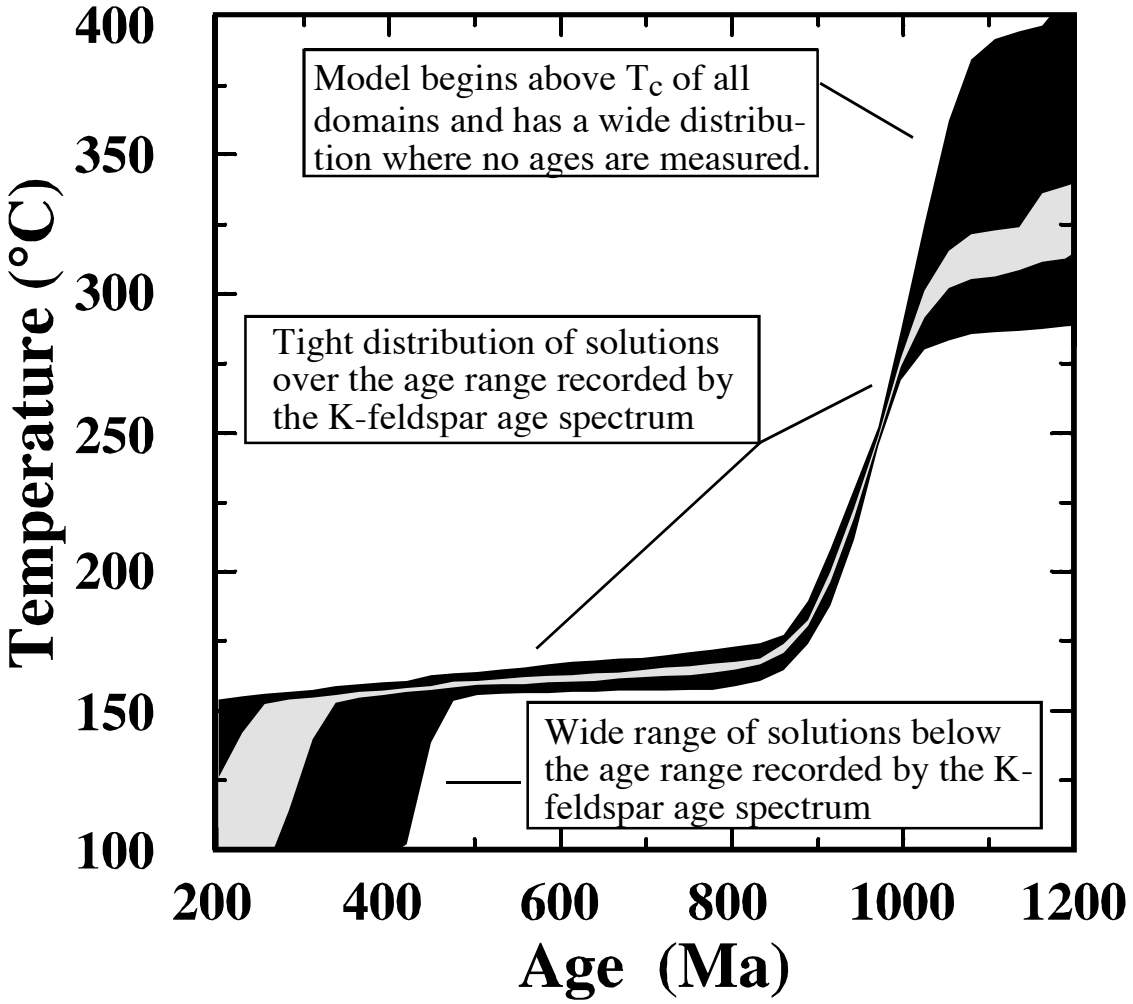

Fig. 4. Thermal histories from monotonic models. Diagram represents contoured results of thermal histories that yield calculated age spectra that match a measured age spectrum. This model only allows the sample to cool from an initially high temperature. The grey band is the 90% confidence interval of the mean, whereas the black band is the 90% confidence of the entire distribution. Large uncertainties in time-temperature space occur where there is either poor agreement between the model and measured data, or more commonly in the age regions that are younger or older than the measured data.

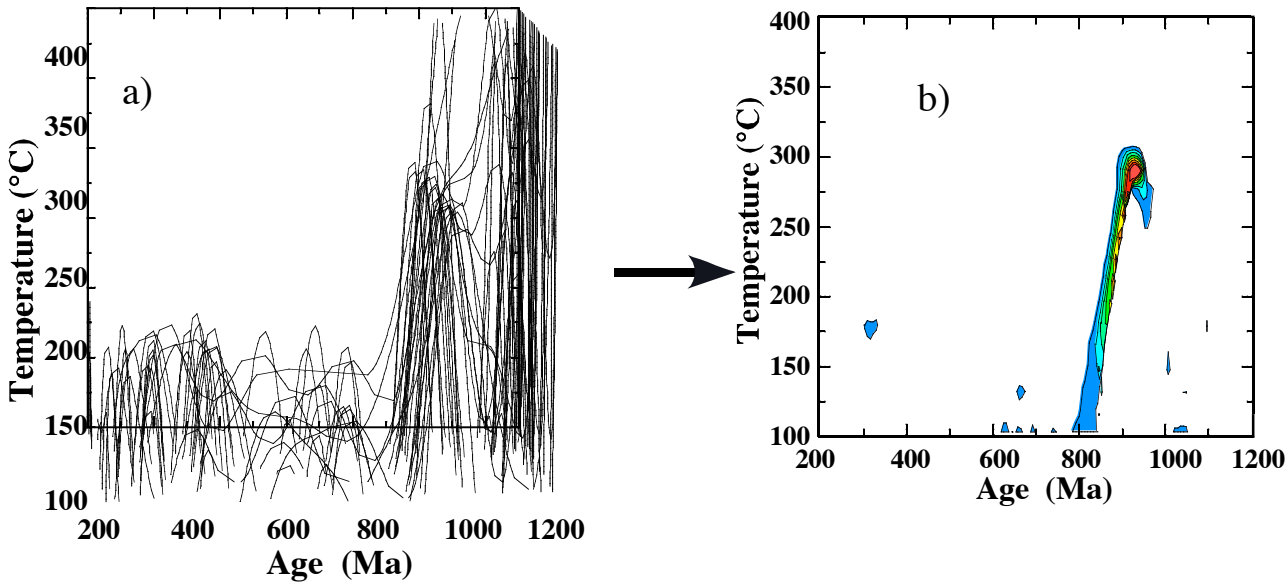

Fig. 5. Thermal histories from unconstrained models. Unconstrained thermal histories incorporate models allowed to accommodate possible reheating events. 5a, Essentially all acceptable models require the sample to be near 275°C at about 950 Ma followed by cooling soon after. Later thermal perturbations cause minor argon loss. 5b, Contoured data of all individual solutions constructed by determining the percentage of solutions that fall within discrete time-temperature bins. Warm colors reflect the highest density of solutions.